The Navball as an Intuitive Avionic Instrument for Lunar Landings

Miguel Neves*
German Aerospace Center (DLR), Münchener Straße 20, 82234 Weßling, Germany

During all six successful Apollo landings, the piloting crew seized control of the lunar lander and landed manually. Intuitive avionic instruments are required for a safe and precise manual landing on the Moon surface as a contingency scenario. In this paper the concept of the Navball is introduced as the main avionic instrument for manually landing on the Moon. Firstly, telemetry data that is required to safely and manually land on the lunar surface is listed and discussed. How to map the telemetry data onto the Navball using planetary references is then discussed in detail. The mechanisms of why the Navball helps to intuitively and safely land are explained. Different users, including an ESA astronaut, tested the Navball successfully, while repeatedly performing a lunar landing on the German Aerospace Center's (DLR) Robotic Motion Simulator (RMS) in a newly developed Human-In-The-Loop controlled lunar landing simulation.

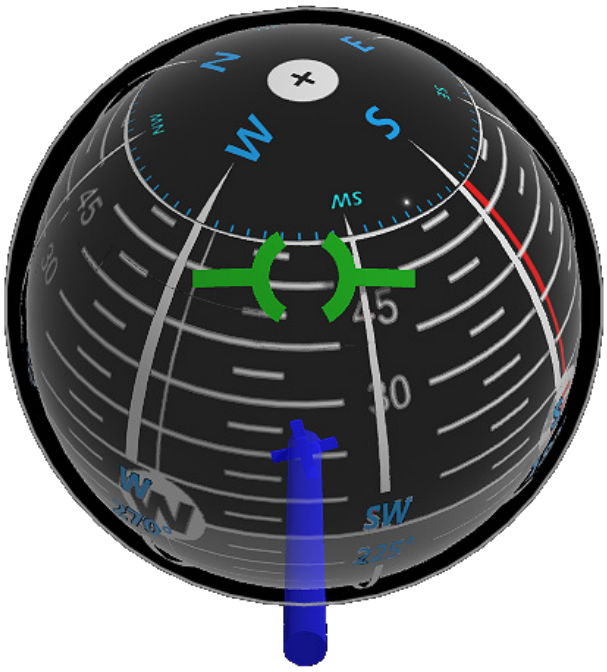

Fig. 1 The Navball.

*Research Assistant, Institute of Robotics and Mechatronics (RM), miguel.neves@dlr.de

I. Introduction

Mankind first stepped on the Moon on July 20, 1969 with the Apollo 11 National Aeronautics and Space Administration (NASA) Mission [1] starting thus a new era of crewed exploration of the Moon. Apollo 17, having left the Moon on December 14, 1972, marks the end of this era only four years later [2].

The latest efforts from the International Space Exploration Coordination Group (ISECG), comprised of 27 space agencies, through the Global Exploration Roadmap (GER) aims to promote the crewed exploration of the Moon with help of the Lunar Orbital Platform-Gateway (LOP-G), more than five decades after man last stepped on the Moon . The LOP-G station will be initially placed in a Near-Rectilinear Halo Orbit around the Moon. From there the astronauts will depart to land on the south pole of the Moon.

All Apollo Lunar Landers (LLs) featured on-board Guidance, Navigation and Control (GNC) systems that automatically piloted them towards their target landing location using fuel optimized strategies. However, "*in each of the six Apollo landings, the astronaut in command seized control from the computer and landed with his hand on the stick*" [3, p. 6].

The Navball is introduced as an avionic instrument designed to aid astronauts on manually landing safely onto the lunar surface. It describes how to model the Navball as a digital instrument and why it is very useful to aid in a manual landing scenario on the Moon. Describing how to model the Navball mechanically is out of the scope of this paper.

II. The Navball

The Navball is an avionic instrument used for navigation in space. Its origins trace back to advancements in inertial navigation systems during the mid-20th century. An early version of the Navball was used in the Apollo program under the name Flight Director Attitude Indicator (FDAI) *, and is visible in Fig. 2. The Navball was later made popular via Kerbal Space Program (KSP), a space flight simulation video game†, as illustrated in Fig. 3.

The Navball represents a mix of various avionic instruments in one while adding features not available in any other avionic instrument. At the base of its concept is a rotating globe with information overlaid on top of it.

Fig. 2 NASA's Flight Director Attitude Indicator (FDAI)

Fig. 3 Kerbal Space Program's Navball.

The Navball's globe features:

1) Longitude lines (vertically) - Also known as meridians, are imaginary vertical lines that run from the North Pole to the South Pole. Longitude is measured in degrees [°] ranging from 0° at the Prime Meridian to 180° east or west.
2) Pitch lines (horizontally) - Horizontal lines that display the current pitch. Pitch is measured in degrees [°] ranging from 0° at the artificial horizon line to 90° at the poles(north or south).
3) Cardinal directions, or cardinal points - the four main compass directions: north (N), south (S) , east (E), and west (W) and its compound directions such as north-east (NE), north-west (NW), south-east (SE) and south-west (SW)

*`https://www.nasa.gov/history/afj/ap16fj/01popup_fdai.html`, Accessed 15-November-2024

†`https://wiki.kerbalspaceprogram.com/wiki/File:Navball.png`, Accessed 15-November-2024

4) The sky - The top half of the instrument is blue to represent the sky
5) The horizon line - separating the sky from the ground
6) The ground - The bottom half is brown to represent the ground

Marine globe compasses, as illustrated in Fig. 14, are avionic instruments that feature cardinal directions and Longitude lines projected onto a globe that rotates hydrostatically. Inclinometers, as illustrated in Fig. 15, are avionic instruments that display the current roll and pitch angles of a vehicle. Artificial horizon gauges, as illustrated in Fig. 16, expand the information provided by inclinometers by adding the current yaw angle.

In its essence a Navball is a marriage between a marine globe compass and an artificial horizon gauge.

Multiple markers can be Juxtaposed on top of the Navball's globe. A breakdown list of the Navball's markers follows:

1) **Level Indicator** (Fig. 13): The level indicator marker (also sometimes called a pitch/roll/yaw level indicator) is used to determine the spacecraft's orientation relative to a planet's local horizon.
2) **Prograde** (Fig. 4): The prograde marker indicates the direction the spacecraft is currently traveling relative to its reference frame. Aligning the level indicator marker with the prograde marker ensures motion along the current trajectory.
3) **Retrograde** (Fig. 5): The retrograde marker shows the direction directly opposite to the spacecraft's motion. Aligning with this marker and firing thrusters slows down the spacecraft relative to its trajectory.
4) **Radial in** (Fig. 6): The radial in marker points toward the center of the celestial body that is being orbited. Aligning with this marker points the spacecraft toward the central body.
5) **Radial out** (Fig. 7): The radial out marker points away from the center of the celestial body that is being orbited. Aligning with this marker points the spacecraft away from the central body.
6) **Normal** (Fig. 8): The normal marker points in the direction that is perpendicular to the orbital plane of the spacecraft or celestial body. Aligning the spacecraft with the Normal marker ensures that thrust is applied in the correct direction to increase inclination.
7) **Anti-Normal** (Fig. 9): The anti-normal marker points downward relative to the orbital plane, opposite to the Normal direction. It is perpendicular to both the orbital path (prograde/retrograde) and the radial directions (radial in/out). Aligning the spacecraft with the Anti-Normal marker ensures that thrust is applied in the correct direction to reduce inclination.
8) **Maneuver** (Fig. 10): The maneuver icon represents the direction the spacecraft must align with to execute a planned maneuver.
9) **Target Prograde** (Fig. 11): The target prograde icon points in the direction of the relative motion of a target object. Aligning with this marker ensures the spacecraft is moving toward the target along its relative velocity vector
10) **Target Retrograde** (Fig. 12): The target retrograde marker represents the direction opposite to the relative motion of a target object. Aligning the spacecraft with this marker ensures that thrust is applied in the opposite direction of your current relative velocity, slowing your approach to the target.

Fig. 4 KSP prograde marker.

Fig. 5 KSP retrograde marker.

Fig. 6 KSP radial-In marker.

Fig. 7 KSP radial-out marker.

Fig. 8 KSP normal marker.

Fig. 9 KSP anti-normal marker.

Fig. 10 KSP maneuver marker.

Fig. 11 KSP target prograde marker.

Fig. 12 KSP target retrograde marker.

Fig. 13 KSP level indicator.

Fig. 14 A generic marine globe compass.

Fig. 15 A generic inclinometer.

Fig. 16 An example of an artificial horizon gauge.

Source: [4]

III. Modeling a Navball

It is possible to model the Navball in various manners. This chapter describes how to model the Navball as a digital instrument. The Navball was implemented and tested using Modelica as its modeling language for this paper.

A. Multi-Body Simulation using Modelica

Modelica is an object-oriented modeling language that enables the modeling of complex multi-domain physical systems. It was introduced in [5–7] and supports mechanical, electrical, thermal, control and process-oriented subsystems and components in one simulation model. The Modelica Association provides the Modelica Standard Library (MSL) [8] containing multi-physical models, including multi-body components which can be used as base components for multi-body systems.

B. Visuals

As mentioned in section II, the Navball's globe was fitted with latitude and inclination lines and cardinal directions. The top hemisphere was colored black to represent the lunar sky, whereas the bottom hemisphere was colored grey to represent the lunar soil. The choice of colors for both hemispheres makes it more intuitive for the user as it coincides with the colors of the Moon, although a stronger color contrast could be more favorable. Fig. 17 illustrates the choice of colors used for this paper's Navball.

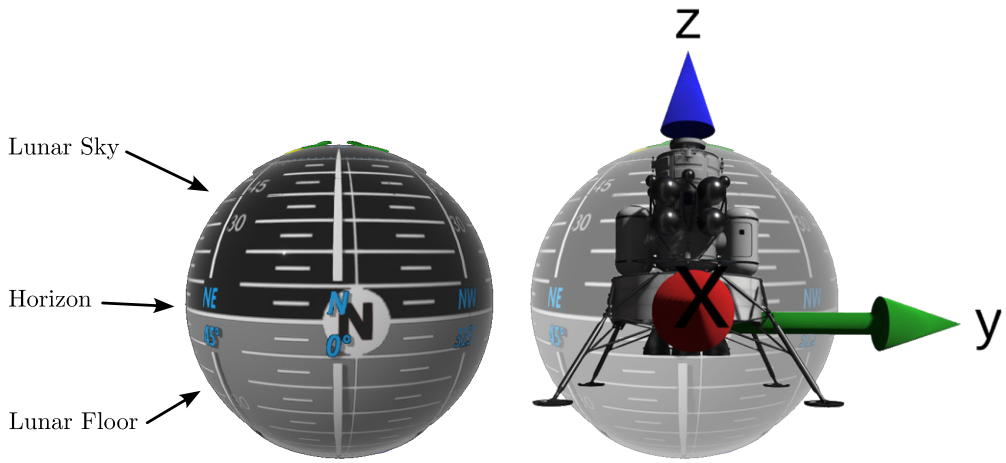

Fig. 17 Side view of the level indicator orientation as it is mapped to the Lunar Lander's (LL's) orientation. The top (black) half hemisphere represents the lunar sky. The bottom (grey) half hemisphere represents the lunar floor.

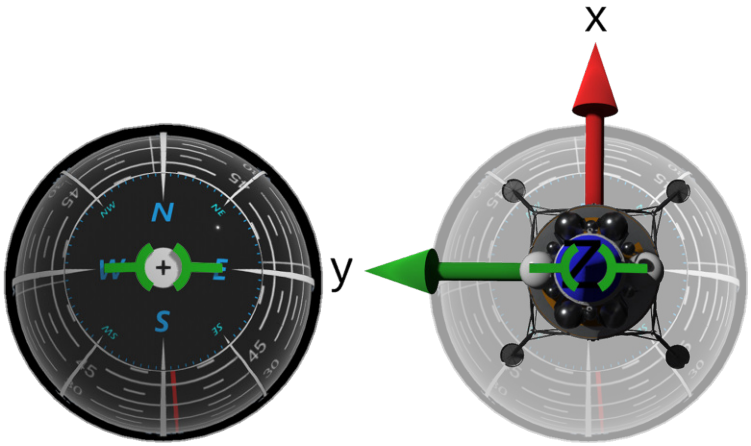

Fig. 18 Top view of the level indicator orientation as it is mapped to the LL's orientation. The indicator marker is aligned with the top of the LL.

C. Choice of Markers

Out of the 10 different markers implemented in the KSP's Navball, three were chosen that allow for a safe lunar landing: The Level Indicator marker, the prograde marker and the retrograde marker as illustrated in Fig. 20. Holograms in the same color as the markers, as illustrated in Fig. 1, were added to all the markers except for the indicator marker as it helps the user to understand where the markers are in the Navball's 3D model sphere. Chapter IV details why these three markers were chosen.

D. Coordinate Systems Needed

Reference systems on the moon are usually described with the following coordinate systems, whose axis allocation is given in Table 1:

1) A global Moon Centered Inertial (MCI) coordinate system.
2) A rotating Planet Centered Planet Fixed (PCPF) coordinate system, that is derived from the MCI coordinate system using the Moon's angular velocity (w_M).
3) East-North-Up (ENU) coordinate systems, that provide coordinate frames that are tangential to the Moon's surface, at a given distance from the Moon's center. ENU frames are aligned with the PCPF coordinate system

and rotate with the Moon.

Fig. 19 shows an overview of the MCI, PCPF and ENU planet coordinate systems.

Table 1 Planet Coordinate System Axis Allocation.

Coordinate System	x axis allocation	y axis allocation	z axis allocation
MCI	-	-	North
PCPF	-	-	North
ENU	East	North	Up

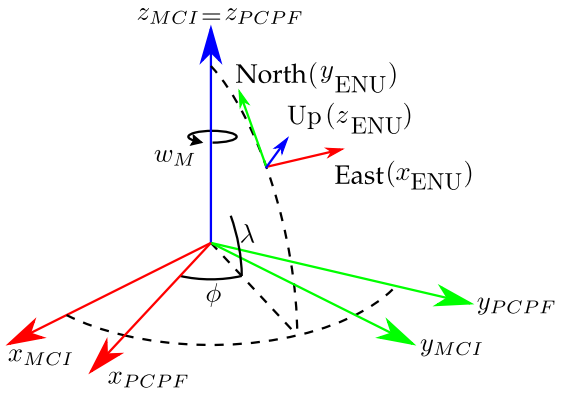

Fig. 19 Overview of the MCI, PCPF and ENU planet coordinate systems.

Source: modified from [9]

E. Telemetry Data

Three telemetry data elements are required as inputs to the Navball:

1) A reference of where up is: By mapping the up vector to the $\vec{U}p$ vector and either the $\vec{E}$ vector to a tracked East coordinate direction or the $\vec{N}$ vector to a tracked North coordinate direction an ENU coordinate frame can be generated. We call this reference frame $\mathbf{R}_{ENU0}(t)$.
2) How the LL is currently oriented: This could be provided by a gyroscope. We call this reference frame $\mathbf{R}_{Body0}(t)$.
3) The current velocity vector of the LL measured in an ENU reference frame: A radar-based signal could be used to track the LL's velocity relative to the lunar soil. Since the $\mathbf{R}_{ENU0}(t)$ frame is available, mapping a measured velocity to the ENU frame is a simple task. We call this measured vector $\vec{v}_{\text{ENU}}(t)$.

F. Kinematic Modeling of the Markers

Let $\mathbf{R}_{BA}$ denote the rotation matrix from frame A to frame B. The compound rotation from frame A to frame B and then from frame B to frame C is then defined as:

$$\mathbf{R}_{CA} = \mathbf{R}_{CB} \cdot \mathbf{R}_{BA} \tag{1}$$

Fig. 20 presents a diagram of the various kinematic operations required to orient the Navball's globe and the markers. $\mathbf{R}_{ENU0}(t)$, $\mathbf{R}_{Body0}(t)$ and $\vec{v}_{\text{ENU}}(t)$ must be available as input variables.

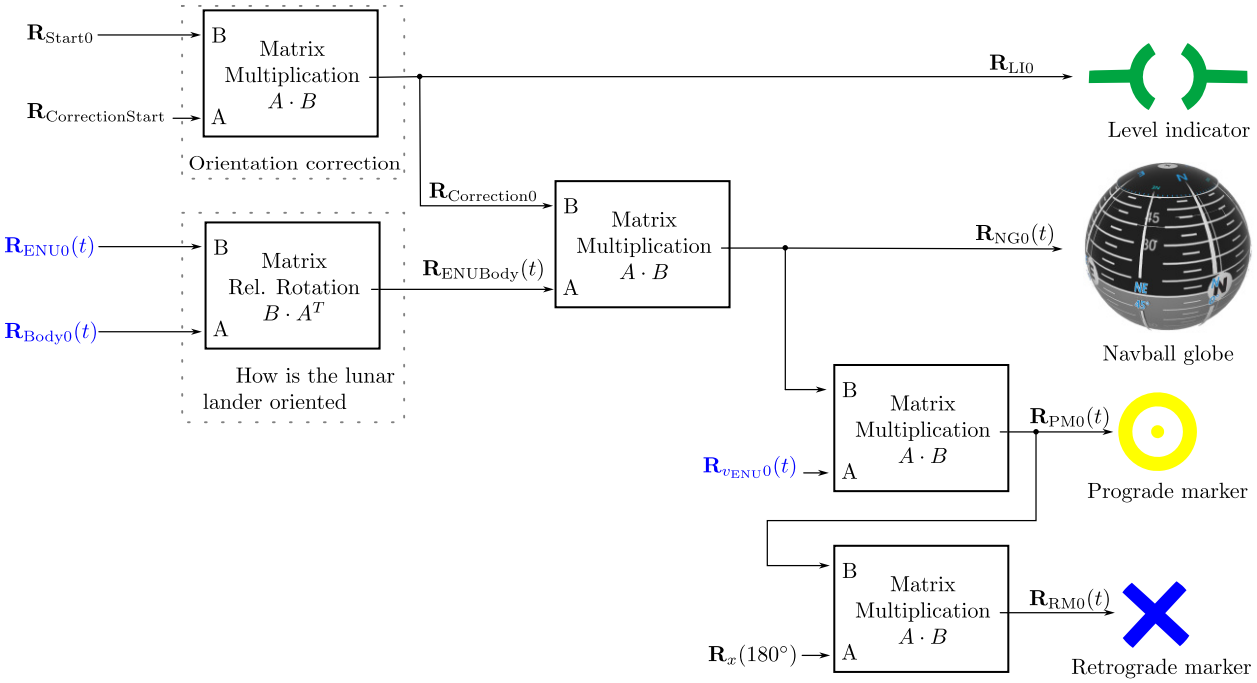

Fig. 20 Kinematic diagram of the Navball's globe and its markers. Rotation matrices in blue represent input data.

To correct or adjust any starting orientation of the Navball ($\mathbf{R}_{Start0}$) to a desired orientation for a better visual experience an orientation correction coordinate frame is introduced as $\mathbf{R}_{CorrectionStart}$. The resulting coordinate frame from the orientation correction operation is named $\mathbf{R}_{Correction0}$ and is obtained by Eq. 2.

$$\mathbf{R}_{Correction0} = \mathbf{R}_{CorrectionStart} \cdot \mathbf{R}_{Start0} \tag{2}$$

To calculate how the LL is oriented relative to the lunar soil the relative rotation between $\mathbf{R}_{Body0}(t)$ and $\mathbf{R}_{ENU0}(t)$ is needed. The resulting coordinate frame from this correction is named $\mathbf{R}_{ENUBody}(t)$ and is obtained by Eq. 3.

$$\mathbf{R}_{ENUBody}(t) = \mathbf{R}_{ENU0}(t) \cdot \left(\mathbf{R}_{Body0}(t)\right)^T \tag{3}$$

1. Level Indicator

The Level Indicator stays permanently upright while the Navball's globe rotates around it. This makes reading easier, as the Level Indicator always faces the screen.
The kinematic chain required for the Level Indicator is:

$$\mathbf{R}_{LI0} = \mathbf{R}_{Correction0} \tag{4}$$

2. Navball Globe

The Navball's globe rotates around the Level Indicator. To project the current roll, pitch and yaw angles of the LL onto the Navball's globe we compute the relative Rotation between the $\mathbf{R}_{ENU0}(t)$ and the $\mathbf{R}_{Body0}(t)$ coordinate frames. If the $\mathbf{R}_{Body0}(t)$ coordinate frame is exactly the same as the $\mathbf{R}_{ENU0}(t)$, the globe is not rotated, with its upper hemisphere aligned with the Level Indicator, as visible in Fig. 18.
The kinematic chain required for the Navball's globe is:

$$\mathbf{R}_{NG0}(t) = \mathbf{R}_{ENUBody}(t) \cdot \mathbf{R}_{Correction0} \tag{5}$$

$$\mathbf{R}_{NG0}(t) = \mathbf{R}_{ENU0}(t) \cdot \left(\mathbf{R}_{Body0}(t)\right)^T \cdot \mathbf{R}_{CorrectionStart} \cdot \mathbf{R}_{Start0} \tag{6}$$

3. Prograde Marker

The prograde vector rotates with the Navball's globe. As a result, its kinematic chain will be built upon the kinematic chain for the Navball's globe .

$$\mathbf{R}_{v_{\text{ENU}}0}(t)\,[3,:] = \frac{\vec{v}_{\text{ENU}}(t)}{\left\|\vec{v}_{\text{ENU}}(t)\right\|} \quad \text{(Z axis)} \tag{7}$$

$$\mathbf{R}_{v_{\text{ENU}}0}(t)\,[2,:] = \frac{\mathbf{R}_{v_{\text{ENU}}0}(t)\,[3,:] \times \mathbf{R}_{ENU0}(t)\,[1,:]}{\left\|\mathbf{R}_{v_{\text{ENU}}0}(t)\,[3,:] \times \mathbf{R}_{ENU0}(t)\,[1,:]\right\|} \quad \text{(Y axis)} \tag{8}$$

$$\mathbf{R}_{v_{\text{ENU}}0}(t)\,[1,:] = \frac{\mathbf{R}_{v_{\text{ENU}}0}(t)\,[2,:] \times \mathbf{R}_{v_{\text{ENU}}0}(t)\,[3,:]}{\left\|\mathbf{R}_{v_{\text{ENU}}0}(t)\,[2,:] \times \mathbf{R}_{v_{\text{ENU}}0}(t)\,[3,:]\right\|} \quad \text{(X axis)} \tag{9}$$

We need to build a coordinate frame with $\vec{v}_{\text{ENU}}(t)$ as its Z axis. To do so, $\vec{v}_{\text{ENU}}(t)$ is firstly normalized to the length of 1, as we are only interested in the direction of the $\vec{v}_{\text{ENU}}(t)$ vector and not its varying length (Eq. 7). The normalized $\frac{\vec{v}_{\text{ENU}}(t)}{\left\|\vec{v}_{\text{ENU}}(t)\right\|}$ vector is then attributed to the Z axis of the $\mathbf{R}_{v_{\text{ENU}}0}(t)$coordinate frame.
By using the cross product between the previously normalized Z axis of the $\mathbf{R}_{v_{\text{ENU}}0}(t)$coordinate frame and the X axis of the $\mathbf{R}_{ENU0}(t)$ coordinate frame we generate the Y axis of the $\mathbf{R}_{v_{\text{ENU}}0}(t)$coordinate frame (Eq. 8).
Finally, the X axis of the $\mathbf{R}_{v_{\text{ENU}}0}(t)$coordinate frame is generated by calculating the cross product between its previously normalized Y and Z axis (Eq. 9).
The kinematic chain required for the prograde marker is:

$$\mathbf{R}_{PM0}(t) = \mathbf{R}_{v_{\text{ENU}}0}(t) \cdot \mathbf{R}_{NG0}(t) \tag{10}$$

$$\mathbf{R}_{PM0}(t) = \mathbf{R}_{v_{\text{ENU}}0}(t) \cdot \mathbf{R}_{ENU0}(t) \cdot \left(\mathbf{R}_{Body0}(t)\right)^T \cdot \mathbf{R}_{CorrectionStart} \cdot \mathbf{R}_{Start0} \tag{11}$$

4. Retrograde Marker

The retrograde vector rotates with the Navball's globe, but in the negative direction of the prograde vector. Consequently, its kinematic chain is built on the kinematic chain for the prograde marker and supplemented by a 180° rotation around its X axis.

$$\mathbf{R}_x(180^\circ) = \begin{bmatrix} 1 & 0 & 0 \\ 0 & -1 & 0 \\ 0 & 0 & -1 \end{bmatrix} \tag{12}$$

The kinematic chain required for the retrograde marker is:

$$\mathbf{R}_{RM0}(t) = \mathbf{R}_x(180^\circ) \cdot \mathbf{R}_{PM0}(t) \tag{13}$$

$$\mathbf{R}_{RM0}(t) = \mathbf{R}_x(180^\circ) \cdot \mathbf{R}_{v_{\text{ENU}}0}(t) \cdot \mathbf{R}_{ENU0}(t) \cdot \left(\mathbf{R}_{Body0}(t)\right)^T \cdot \mathbf{R}_{CorrectionStart} \cdot \mathbf{R}_{Start0} \tag{14}$$

IV. Navball based Moon landing

The last phase of a lunar landing [‡] is when the piloting astronaut acquires visuals of the landing site and is then able to switch the Guidance, Navigation and Control (GNC) system from auto-pilot to semi-manual, to perform the landing "manually" [3, p. 6]. During this phase the LL follows a planar path towards the lunar soil [10, p. 3], as illustrated in Fig. 22. An analysis of the forces acting on a LL during a planar landing trajectory helps to understand why the Navball is very useful for a manual lunar landing.

Fig. 21 shows a diagram of the forces acting on the LL during a lunar descent. $\mathbf{f}_b(t)[\text{N}]$ represents the booster force, $\mathbf{f}_g[\text{N}]$ the gravity force, $\mathbf{v}(t)[\text{m/s}]$ the velocity vector (prograde) and $-\mathbf{v}(t)[\text{m/s}]$ the negative velocity vector (retrograde). $\vartheta[\text{rad}]$ represents the LL's pitch angle. Since the Moon is deprived of any atmosphere, there is no gas friction and no wind force acting on the LL. The LL must be oriented so that it can counter both the acceleration of

[‡]Named Low Gate and Soft Landing Phase in the Apollo Moon landing missions

gravity pulling it towards the lunar soil and its lateral speed in order to reach a landing target safely. $\mathbf{f}_b(t)\,[\mathrm{N}]$ can be decomposed into its Z and X axes components, $f_{b_z}(t)\,[\mathrm{N}]$ and $f_{b_x}(t)\,[\mathrm{N}]$ respectively:

$$\mathbf{f}_b(t) = \langle f_{b_x}(t), 0, f_{b_z}(t) \rangle\,[\mathrm{N}] \tag{15}$$

$-\mathbf{v}(t)\,[\mathrm{m/s}]$ represents the LL'S velocity vector (prograde) and can also be decomposed into its Z and X axes components, $v_z\,[\mathrm{m/s}]$ and $v_x\,[\mathrm{m/s}]$ respectively:

$$\mathbf{v}(t) = \langle v_x(t), 0, v_z(t) \rangle\,[\mathrm{m/s}] \tag{16}$$

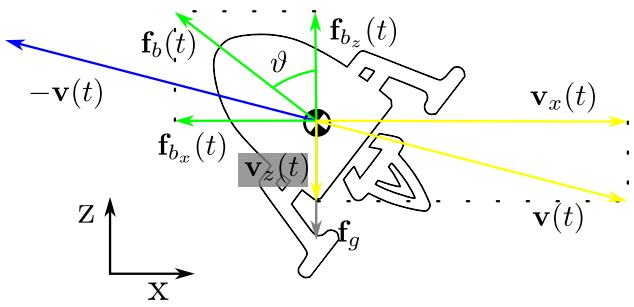

Fig. 21 Force diagram of the forces acting on the LL during a lunar descent.

Through Fig. 21 it is visible that both the descent and lateral speeds depend on the pitch angle $\vartheta\,[\mathrm{rad}]$ of the LL and how much of the booster force $\mathbf{f}_b(t)\,[\mathrm{N}]$ is being used. If the pitch angle is set to $\vartheta = 0\,\mathrm{rad}$, the LL is able to counter its descent speed with its entire booster force. In this scenario, the LL won't crash vertically against the lunar soil, but will have too much lateral speed and will roll on the lunar soil the moment it makes contact. To set the pitch angle to $\vartheta = 0\,\mathrm{rad}$, the level indicator marker is aligned to the top dead center of the Navball, as illustrated in Fig. 18.
If the pitch angle is set to $\vartheta = \pi/2$ rad, the LL is able to counter its lateral speed with its entire booster force. In this scenario, the LL won't have any lateral speed but will crash against the lunar soil due to its accelerating descent speed. To set the pitch angle to $\vartheta = \pi/2$ rad, the level indicator marker is aligned with the horizon line of the Navball.

It is possible to set the pitch angle so that the LL's booster acts in a direction that reduces its velocity by aligning the indicator marker with the retrograde marker of the Navball. This approach makes sense as long as the descent speed remains negative and within a safety margin. Note that the force of gravity $\mathbf{f}_g\,[\mathrm{N}]$ will keep pulling the LL towards the lunar soil. If the remaining distance to ground is too small, the LL will crash with the soil before the velocity vector has been canceled entirely.

Fig. 22 presents the general approach for how to manually land on the Moon using the Navball. The indicator marker (in green) is set between the top dead center of the Navball and the retrograde marker (in blue). The Astronaut needs to monitor its descent speed and continuously adjust the pitch and throttle values so that the descent speed remains negative and within a safety margin.

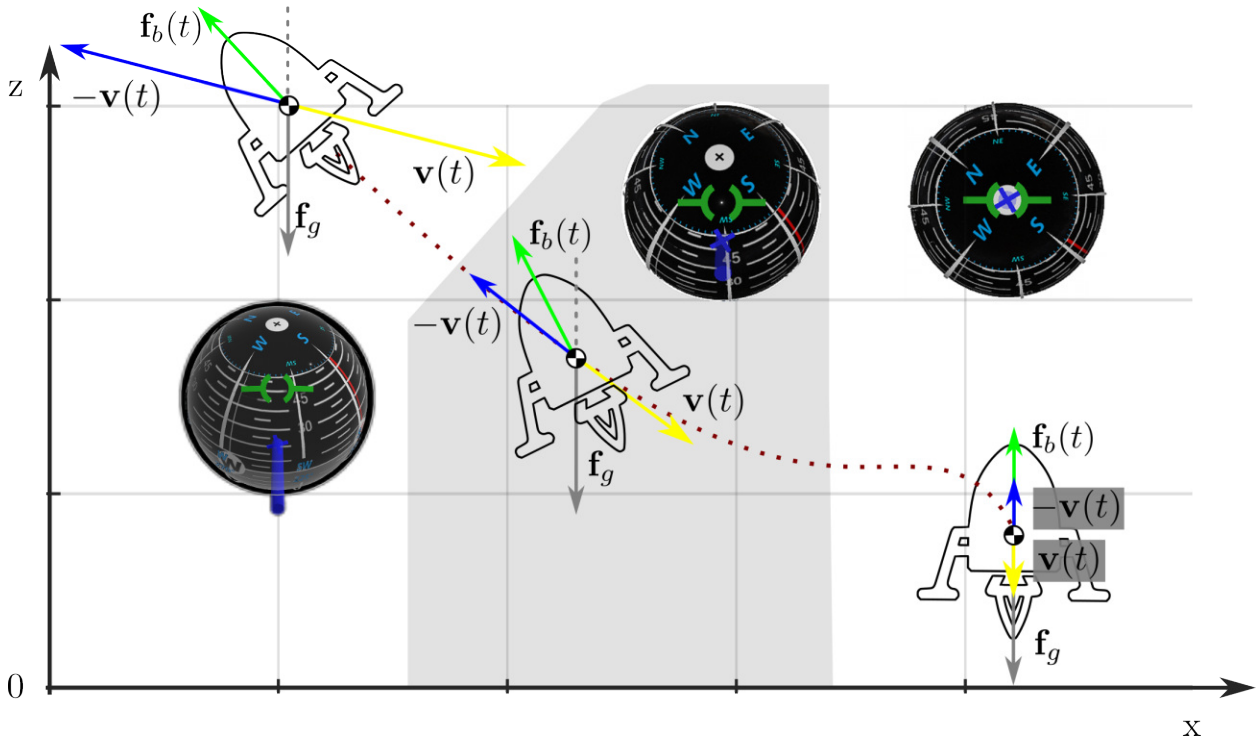

Fig. 22 The general approach for how to manually land on the Moon using the Navball. The green indicator marker is set between the top dead center of the Navball and the blue retrograde marker. Orientation and Throttle values need to be adjusted continually so that the descent speed remains negative and within a safety margin.

Source: modified from [11, p. 64]

V. Validation and Experiment

A. Experiment Setup

1. Motion Simulation System

The Navball was tested in combination with the German Aerospace Center (DLR) Robotic Motion Simulator (RMS) [11–18]. The RMS represents a class of motion simulators being currently developed at DLR. It is based on an industrial 6 Degrees of Freedom (DOF) serial kinematic industrial actuator (i.e. an industrial robot arm) that is mounted onto a 10 m long linear axis forming a redundant 7 Degrees of Freedom (DOF) architecture to induce motion cues onto an attached simulator cell, as illustrated in Fig. 23.

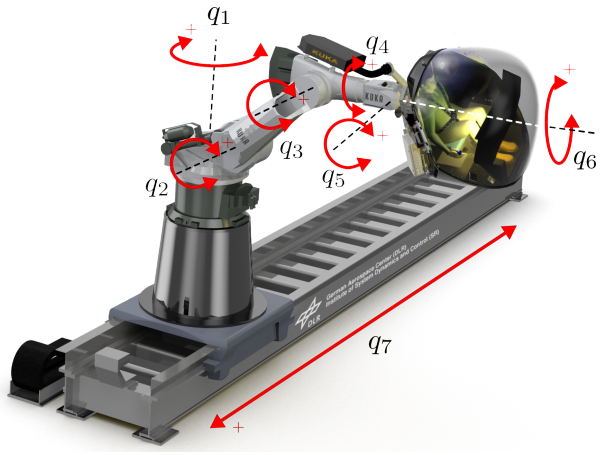

Fig. 23 DLR Robotic Motion Simulator (RMS) overview, showing joint locations and turning directions of the robotic platform.

Fig. 24 Exploded view of DLR RMS's simulator cell showing It's modular design.

2. Simulator Cell

The RMS is fitted with a highly modular simulator cell that can be configured to best serve the simulation purpose intended, as illustrated in Fig. 24. It features sitting modules with instrument bays and different instrument modules that are attachable to the sitting module. The simulator cell is fitted with a stereo-projection system and a multitude of safety devices. The RMS can be used in combination with Virtual Reality (VR) glasses that track the pilot's head position to deliver an immersive VR experience.

For the presented lunar landing scenario, the seating module was configured as shown in Fig. 26. It features three touch-screens that were used to interact with the Human Machine Interface (HMI) software, instruments, a virtual window to the outside, as well as a headset and a surveillance camera for the piloting astronaut. The VR glasses were removed for this experiment and the stereo-projection system was not used. The piloting astronaut had to rely on the HMI, the LL's virtual window to the outside and the motion cues from the RMS in order to land safely.

3. Lunar Lander (LL) Parameters

The Simulated LL is a fictitious vehicle that was never built. Its 3D Model was provided by European Space Agency (ESA) during the project documented in [18]. The model bears a strong resemblance to the Lunar Surface Access Module (LSAM) concept, a study concept from ESA commissioned by NASA and published in [19]. The simulated system has a wet mass of 43 t and a maximum total thrust of 264 kN, provided by four main boosters [§]. For the descent phase the maximum available thrust has been capped to 60% of the maximum total thrust, according to the Apollo 11 landing trajectory [21, p. 3] . Vector thrusting is used for attitude control by gimballing the main thrusters. The landing legs interact with the surface through a detailed contact model.

4. Graphical User Interface (GUI)

The HMI features a Primary Flight Display (PFD)(middle screen), a Navigation Display (ND)(left screen) and a Multi-function Flight Display (MFD) (right screen). The ND features flight data and a safety map [18, p. 4] projected onto of the GNC Camera stream that gives the piloting astronaut the ability to see if the landing site is obstacle free. The MFD features four downward GNC Cameras and the status of the system.
The PFD provides the pilot with a Navball and standard avionic indicators. The final Navball GUI interface can be seen in Fig. 25 and features:

[§]Parameters derived from [19, pp. 23–24] and [20, pp. 10].

- The Navball, in the center.
- A PFD, at the same height as the Navball.
- An altitude rate indicator, left of the Navball.
- An altitude indicator, right of the Navball.
- A ground speed indicator, below the Navball. It Indicates the LL's lateral speed relative to the ground. If the black point is to the right of the center circle the LL is moving to the right. If the the black point is in front of the center circle the LL is moving forwards. If the black point is, in the middle of the center circle, the LL has no lateral speed.
- Propellant remaining indicators, left of the Navball.
- Lander Status. It indicates which of the main boosters is active and whether any landing gear leg has made contact with the ground.
- Status LEDs.
- Main engine thrust indicators.

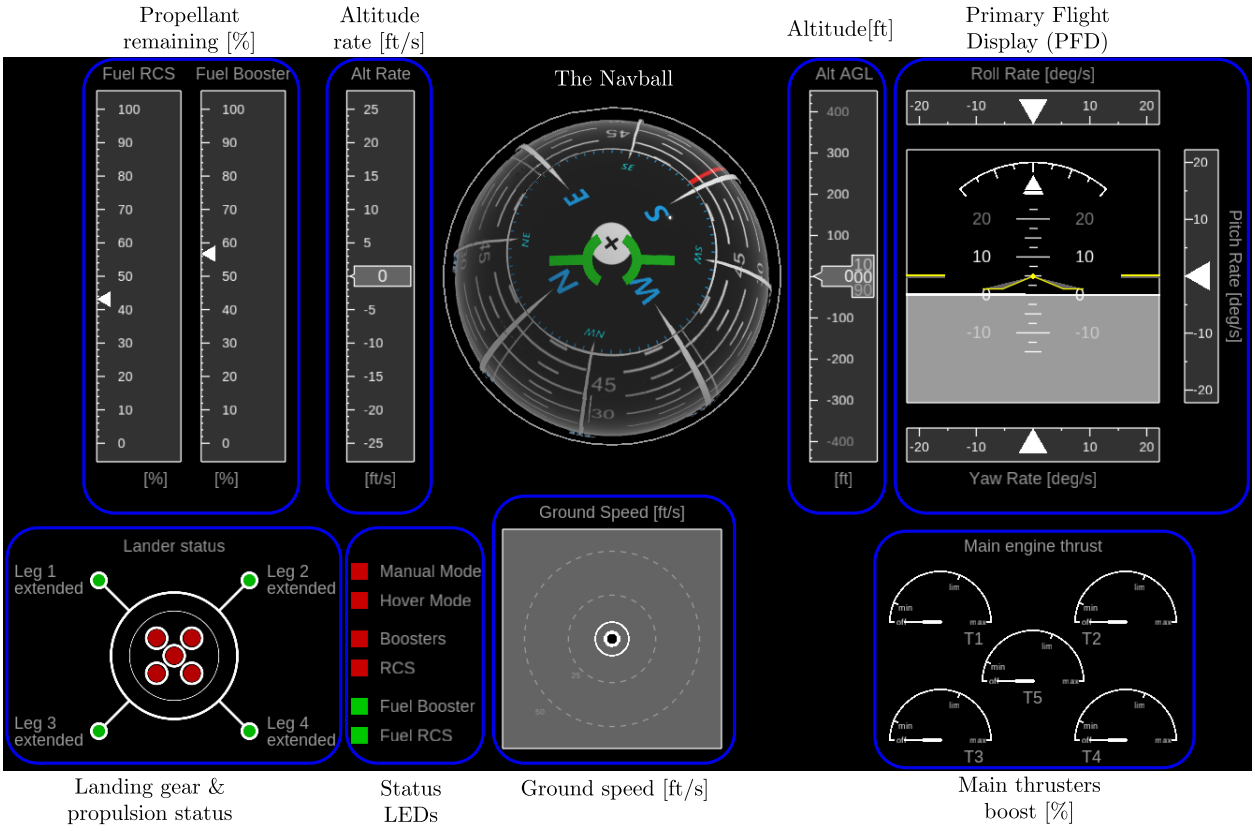

Fig. 25 The Navball GUI. The various instruments available are framed in blue to describe their functions.

5. Instruments

Commercially available Off-The-Shelf (COTS) components were chosen for this experiment. The joystick features 3 active DOFs and the throttle allows for adjustable damping along with buttons that were used as inputs to the simulation.

6. Manual Steering Mode

To simulate a contingency scenario, the pilot steers the LL manually. *Attitude Rate Control* was chosen as the manual control mode for the experiment. Using the Joystick, the pilot inputs the direction of desired rotational motion. This results in a desired angular velocity vector $\boldsymbol{\omega}_d \neq \mathbf{0}$ rad s^{-1} being input from the pilot into the controller. The controller actuates in order to reduce the angular velocity error and starts rotating the lander in the direction input from the pilot. The rotation only stops once the pilot returns the joystick into its 0 position, as $\boldsymbol{\omega}_d = \mathbf{0}$ rad s^{-1}. The main

Fig. 26 Configured seating module for the Human-In-The-Loop (HITL) LL simulation. The top screen acts as a virtual window to the outside. Digital instruments are displayed over the three front screens. A force side-stick and a throttle lever are the main HMI's used to pilot the LL.

advantage of *Attitude Rate Control* is that it takes the actuator complexity away from the pilot:

- Tilting the Joystick forwards results in a forwards pitch rotation.
- Tilting the Joystick backwards results in a backwards pitch rotation.
- Tilting the Joystick to the right results in a roll rotation to the right.
- Tilting the Joystick to the left results in a roll rotation to the left.
- Twisting the Joystick to the left results in a yaw rotation to the left.
- Twisting the Joystick to the right results in a yaw rotation to the right.
- Not moving the Joystick results in no rotation of the LL.

7. Visualizing the Environment

For the Moon landing scenery, a high-resolution lunar crater visualization based on DLR's Visualization 2 library [22] has been developed. This environment visualization was displayed on the virtual window inside the capsule (see Fig. 26), allowing the piloting astronaut to further assess the situation and the lander's attitude. The visualization of the environment showing the lander from an outside perspective was also displayed on a screen outside of the RMS for external observers.

B. Moon Landing Experiment

The experiment objectives were simply to survive the last critical seconds of a realistic emergency Moon landing. The final descent phase of the Apollo 11 mission was chosen as a realistic scenario for a contingency Moon landing. A reconstructed landing path for Apollo 11 is available in [11, pp. 58–66] and was used as the reference trajectory for this experiment.

1. Initial Conditions

Parameters required to define a starting state for the LL were derived from [11, pp. 58–66] and are listed in Table 2.

Table 2 Initial Position State Parameters for a LL Simulation Based on the Generated Path for Apollo 11 Moon Landing Descent

Parameter	Description	Value
$\mathbf{r}_i$	Initial position	$\{-1950, 0, 310\}$m
$\mathbf{v}_i$	Initial velocity	$\{74.0, 0, -19.06\}$m/s
$\frac{\mathbf{f}_{bi}}{\|\mathbf{f}_{bi}\|}$	Initial booster force direction	$\{-0.5623, 0.0000, 0.8269\}$N
Thr_i	Initial throttling %	57.23%

Source: [11]

The LL's starting position from the landing target was defined as $\mathbf{r}_i = \langle -1950, 0, 310 \rangle$m. The starting pitch angle ϑ_i is given by the x and z components of $\frac{\mathbf{f}_{bi}}{\|\mathbf{f}_{bi}\|}$:

$$\arctan(\vartheta_i) = \frac{0.8269}{-0.5623} \tag{17}$$

$$\vartheta_i \approx -55.8^\circ \tag{18}$$

2. Experiment Evaluation

An emergency Moon landing is deemed safe if the following criteria are met, as the LL touches the lunar soil:

- Terrain Safety: Valid if the landing location is green (safe) in the safety map. Invalid if the landing location is red (unsafe) in the safety map.
- Vertical Speed (v_z):

$$-5\,\mathrm{m/s} < v_z < 0\,\mathrm{m/s} \tag{19}$$

  The final descent speed has to stay within the envelope to be considered valid.
- Lateral Speed (v_x) and (v_y):

$$0\,\mathrm{m/s} < |v_x| < 5\,\mathrm{m/s} \tag{20}$$

$$0\,\mathrm{m/s} < |v_y| < 5\,\mathrm{m/s} \tag{21}$$

  The final lateral speeds have to stay within the envelope to be considered valid.

3. Experiment Procedure

Firstly the pilot is briefed on how to land on the Moon using the Navball, as described in Chapter IV, and the provided GUI. The Simulation begins with the LL with an initial velocity $\mathbf{v}_i[\mathrm{m/s}]$, at an initial distance from the landing target $\mathbf{r}_i$ while it is pitched backwards by the initial tilt angle ϑ_i. The pilot must then set the pitch angle so that the LL's booster acts in a direction that reduces its velocity. The pilot can either use the Navball or the PFD as its main landing instrument. For a Navball based landing, the pilot has to reduce the LL's velocity by tilting the Joystick so that the Navball's green indicator marker is set between the top dead center of the Navball and the blue retrograde marker.
The descent speed needs to be constantly monitored and the pitch and throttle values need to be constantly adjusted so that the descent speed remains negative and within a safety margin:

- If the descent speed exceeds the limits given by Eq. 19, the throttle needs to be adjusted.
- If the lateral speed exceeds the limits given by Eq. 20 and Eq. 21, the orientation needs to be adjusted.

The pilot needs to verify on the visibility map if the soil underneath the LL is safe to land and correct accordingly. Normally the visibility map is colored green where the lunar soil is safe to land and red where a landing is not safe [18, p. 4]. The amount of propellant available is finite, limiting the maximum possible duration of the experiment. If the LL's propellant runs out before the LL lands, it is not possible to reduce the descent speed and the pilot will crash.
A Moon landing is successful when the criteria for a safe lunar landing, as listed in Chapter V.B.2, are met as the LL touches the lunar soil.

C. Concept and Validation

The concept of whether or not the Navball can be used as an intuitive avionic instrument for lunar landings was tested.

By using standardized avionic instruments with the exception of the Navball, the Pilot was able to focus primarily on the Navball if desired. The aim here was to achieve a successful landing and see what additional factors needed to be taken into account.

Different users with and without previous flight experience, including ESA's Astronaut *Roberto Vittori*, proceeded with the experiment, as described in Chapter V.B.3, using the provided GUI. Landing on the Moon manually is a demanding task. For this reason, users need to have a certain amount of previous experience to be able to land safely. As a result, users were able to repeat the experiment as often as they desired.

The users that relied on the Navball as its main landing instrument were able to successfully land on the moon within a few trials. On the other hand, users relying on the PFD as its main landing instrument didn't manage to land on the moon while meeting the safe landing criteria highlighted in Section V.B.2. The most common issue they encountered was that the propellant ran out before a safe landing was achieved.

It is to note that this experiment was an early-stage concept study and no user-study was carried out, only an experiment with a small group of test users. Nonetheless in the experiment the Navball was intuitivelly used as an avionic instrument to land on the Moon safely.

VI. Conclusion

By integrating critical telemetry data with intuitive visualizations based on planetary references, the Navball enables precise and safe piloting under contingency scenarios. The Concept was validated through testing, on the German Aerospace Center's Robotic Motion Simulator, where diverse users, including an ESA astronaut, tested the use of the Navball while trying to safely land on the lunar soil. The experiment acts as an early-stage concept study of effectiveness of the Navball as an intuitive avionic device for landing on the Moon. In our experiment, users were unsuccessful at landing on the Moon safely without using the Navball. The experiments also provided an insight into the limitations and weaknesses of the Navball, which could play a major role in future user studies. The Navball in particular and its properties can be expanded as required and help the user to keep their bearings during difficult missions. In further studies other Navball markers should also be considered, such as the maneuver marker to precisely guide the pilot on how to orient the LL for a safe manual landing.

VII. Acknowledgements

The presented work has been internally funded by the German Aerospace Center (DLR). The author thanks the European Space Agency (ESA) for providing the 3D Model of the Lunar Lander (LL) used; In addition, the author thanks the Astronaut Roberto Vittori for testing the use of the Navball while performing the test campaign documented in [23] at DLR.

References

[1] Aeronautics, U. S. N., and Administration, S., *Apollo 11 Mission Report*, Press kit, NASA, 1969. URL `https://www.hq.nasa.gov/alsj/a410/A08_MissionReport.pdf`.

[2] Aeronautics, U. S. N., and Administration, S., *Apollo 17 Mission Report*, Press kit, NASA, 1973. URL `https://www.hq.nasa.gov/alsj/a17/A17_MissionReport.pdf`.

[3] Mindell, D. A., *Digital Apollo: human and machine in spaceflight*, Mit Press, 2011.

[4] Wikipedia, 2024. URL `https://de.wikipedia.org/wiki/K%C3%BCnstlicher_Horizont#/media/Datei:VMS_Artificial_Horizon.jpg`.

[5] Mattsson, S. E., Elmqvist, H., and Otter, M., "Physical System Modeling with Modelica," *Control Engineering Practice*, 1998.

[6] Tiller, M., *Introduction to Physical Modeling with Modelica*, The Springer International Series in Engineering and Computer Science, 2001.

[7] Elmqvist, H., Mattsson, S. E., and Otter, M., "Modelica - An International Effort to Design an Object-Oriented Modeling Language," *Summer Computer Simulation Conference*, 2003.

[8] Otter, M., Elmqvist, H., and Mattsson, S., "The New Modelica MultiBody Library," *Proceedings of the 3rd International Modelica Conference*, 2003.

[9] Briese, L. E., Schnepper, K., and Acquatella, P., "Advanced modeling and trajectory optimization framework for reusable launch vehicles," *2018 IEEE Aerospace Conference*, IEEE, 2018, pp. 1–18.

[10] Bennett, F. V., "Apollo lunar descent and ascent trajectories," *AIAA 8TH AEROSPACE SCI. MEETING*, 1970.

[11] Neves, M., "Human-In-The-Loop Controlled Lunar Landing Simulator," Master's thesis, Technical University of Munich, 2019.

[12] Bellmann, T., Heindl, J., Hellerer, M., Kuchar, R., Sharma, K., and Hirzinger, G., "The DLR robot motion simulator part i: Design and setup," *2011 IEEE International Conference on Robotics and Automation*, IEEE, 2011, pp. 4694–4701.

[13] Bellmann, T., Otter, M., and Hirzinger, G., "The DLR Robot Motion Simulator Part II : Optimization based path-planning," *IEEE International Conference on Robotics and Automation*, 2011. URL `https://elib.dlr.de/71363/`.

[14] Bellmann, T., *Optimierungsbasierte Bahnplanung für interaktive robotische Bewegungssimulatoren*, Verlag Dr. Hut, 2014.

[15] Bellmann, T., and Labusch, A., "Next generation pilot training with robot-based flight simulators," *Flight Simulation Conference 2014: The Future of Flight Training Devices*, edited by R. A. Society, 2015. URL `https://elib.dlr.de/112050/`.

[16] Lombaerts, T., Looye, G., Seefried, A., Neves, M., and Bellmann, T., "Development and concept demonstration of a physics based adaptive flight envelope protection algorithm," *IFAC-PapersOnLine*, Vol. 49, No. 5, 2016, pp. 248–253.

[17] Seefried, A., Pollok, A., Kuchar, R., Hellerer, M., Leitner, M., Milz, D., Schallert, C., Kier, T., Looye, G., and Bellmann, T., "Multi-domain Flight Simulation with the DLR Robotic Motion Simulator," *Spring Simulation Conference 2019*, 2019.

[18] Neves, M., Seefried, A., Bellmann, T., Hagenfeldt, M., Sorbellini, E., Vittori, R., and Ferracina, L., "A Novel Human-in-the-Loop Testing Facility for Space Applications," *2nd International Conference on Flight Vehicles, Aerothermodynamics and Re-entry Missions & Engineering (FAR)*, 2022.

[19] Stanley, D., Cook, S., Connolly, J., Hamaker, J., Ivins, M., Peterson, W., Geffre, J., Cirillo, B., McClesky, C., Hanley, J., et al., "NASA's exploration systems architecture study," *NASA Technical Report*, 2005.

[20] Thangavelu, M., and Mekonnen, E., "Preliminary Infrastructure Development for Altair Sortie Operations," *AIAA SPACE 2009 Conference & Exposition*, 2009, p. 6422.

[21] NASA, "Apollo Command and Service Module - Guidance and control," Tech. rep., National Aeronautics and Space Administration, 1970. URL `https://www.hq.nasa.gov/alsj/CSM19_Stabilization_&_Control_pp189-204.pdf`.

[22] Kümper, S., Hellerer, M., and Bellmann, T., "DLR Visualization 2 Library - Real-Time Graphical Environments for Virtual Commissioning," *14th Modelica Conference*, edited by M. Sjölund, L. Buffoni, A. Pop, and L. Ochel, Modelica Association and Linköping University Electronic Press, 2021, pp. 197–204. URL `https://elib.dlr.de/144780/`.

[23] Born, J., Seefried, A., Neves, M., Asadi, H., and Bellmann, T., "Modified Optimal Motion Cueing Algorithm with Haptic Feedback for Full Motion Simulation for a Reduced Gravity Environment," *2024 International Conference on Space Robotics (iSpaRo)*, IEEE, 2024, pp. 307–314.